APPLYING THREE-COMPONENT RECORDS IN WAVE FIELD SEPARATION

R. DAURES* and P. TARIEL*

In zero-offset Vertical Seismic Profiles, the wave field includes only upgoing and downgoing P-waves having only vertical (Z) components. When the source is offset, the wave field becomes complicated by the presence of converted P–SV-waves different from P-waves by their apparent velocity and their direction of polarization. Seismic is no longer scalar but vectorial, and therefore three-component records are needed.

On the first arrival, the hodograph gives the polarization direction of the P-wave. The polarization direction of P–SV-waves is estimated by assuming a two-to-one P to S velocity ratio. The combined use of a set of axis-changes related to the directions of polarization, and the f–k filtering associated with the apparent velocities allows the separation of the total wave field into the four following types: downgoing P-, upgoing P-, downgoing P–SV- and upgoing P–SV-waves.

1. Introduction

This paper addresses three-component recording (X, Y, Z) in a borehole, assuming gently dipping sedimentation. In the case of zero-offset Vertical Seismic Profiles (VSPs), the P-wave emitted from the surface reaches the reflectors with normal incidence, which does not generate converted waves. The recording of the vertical (Z) component provides full knowledge of the P-wave field. There is only one polarization direction, this being vertical. Seismic is then scalar, and up- and downgoing P-waves are differentiated by their apparent velocities. Many separation algorithms have already been used.

When the source is offset, the wave field becomes more complex. The P-wave emitted from the surface reaches the reflectors with far from normal incidence, and converted waves are generated (P-reflected SV and P-transmitted SV). Several types of waves appear, and each type is characterized by its own polarization direction and its own apparent velocity. Seismic is no longer scalar but vectorial. Complete knowledge of the wave field now requires three-component recording.

The aim is to separate the different types of waves in the (Z, T) domain limited by the times of the first P-arrival and the first S-arrival. We will assume that there are only four significant types of waves:

* Compagnie Générale de Géophysique 91341 Massy, France

— downgoing *P*
— upgoing *P*
— downgoing *P–SV* (*P*-waves converted to *SV* mode through transmission)
— upgoing *P–SV* (*P*-waves converted to *SV* mode through reflection).

On the first arrival, the hodograph gives the polarization direction of the *P*-wave. The polarization direction of *P–SV*-waves is estimated by assuming a two-to-one *P* to *S* velocity ratio.

The combined use of a set of axis-changes related to the directions of polarization, and the *f–k* filtering associated with the apparent velocities, allows the total wave field to be separated into the four following types: downgoing *P*-, upgoing *P*-, downgoing *P–SV*- and upgoing *P–SV*-waves.

There are four stages in this separation:

a) Vector composition of two horizontal components to represent the problem in 2-D.

b) Change in the set of axes according to the polarization direction of downgoing *P*-waves and to its orthogonal direction, with velocity filtering of the *P*-waves on the first component.

HORIZONTAL COMPONENTS

(X , Y)

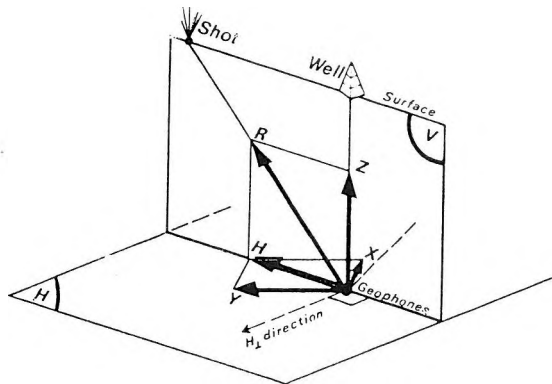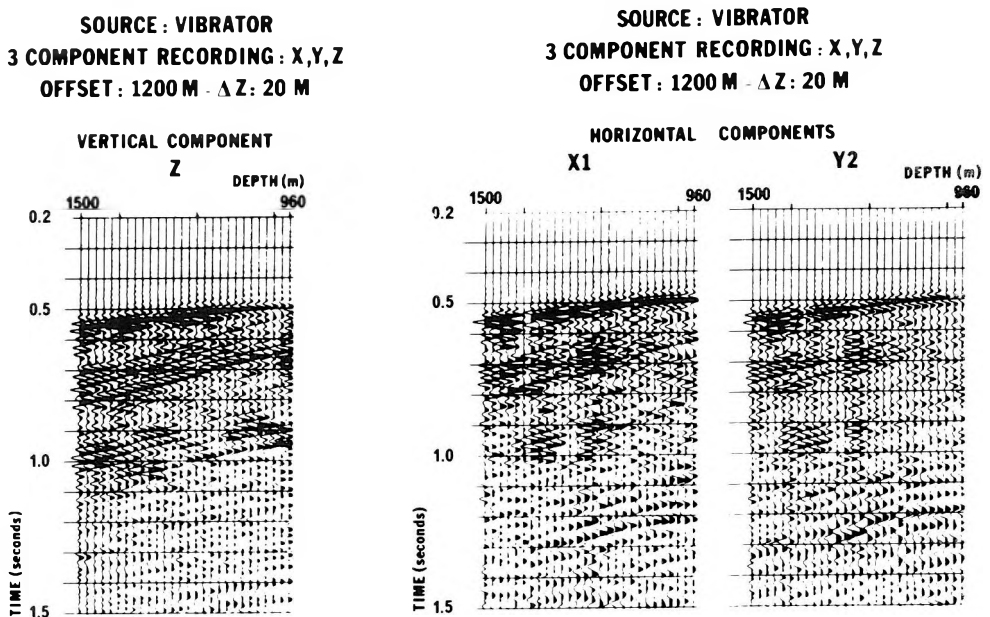## COMPOSITION

3D PROBLEM ⟹ 2D PROBLEM

Fig. 1. Schematic diagram of detector orientation using three-component geophone in a VSP recording survey

1. ábra. Detektor orientáció háromkomponenses geofonnal készített VSP felvétel esetén

Рис. 1. Ориентировка детектора при записи ВСП с использованием трехкомпонентных сейсмоприемников.

c) Second change in the set of axes according to the polarization direction of downgoing *P–SV* waves and to its orthogonal direction, with velocity filtering of the *P–SV* waves on the first component.

d) Separation of upgoing *P*-waves and upgoing *P–SV*-waves by changing the set of reference axes.

Each type of wave usually shows projections on the three-component axes since the projection system is randomly oriented (see *Fig. 1*). The first operation consists of selecting a reference system with one vertical plane containing the source. We then face only a 2-D problem about the couple of components (*Z* and *H*) belonging to that plane *(Fig. 2)*. In order to perform this rotation, the two horizontal components of the initial system are conventionally added so as to maximize the energy of the direct wave. A very weak level of residual energy appears along the perpendicular *H* direction *(Fig. 3)*, which generally confirms the existence of a measurement plane containing most of the energy of the *P*- and *SV*-waves.

SOURCE : VIBRATOR
3 COMPONENT RECORDING : X,Y,Z
OFFSET : 1200 M - Δ Z : 20 M

VERTICAL COMPONENT

SOURCE : VIBRATOR
3 COMPONENT RECORDING : X,Y,Z
OFFSET : 1200 M - Δ Z : 20 M

HORIZONTAL COMPONENTS

Fig. 2. Offset VSP raw data. Three-component well geophone recording: one vertical (left) and two horizontal (right) components

2. ábra. Távoli gerjesztésű VSP felvétel háromkomponensű lyukgeofonnal: egy függőleges (bal oldalon) és két vízszintes (jobb oldalon) komponens

Рис. 2. Запись ВСП с дальним возбуждением с использованием трехкомпонентных скважинных сейсмоприемников: одна компонента вертикальна (на левой стороне), а две другие горизонтальны (на правой стороне).
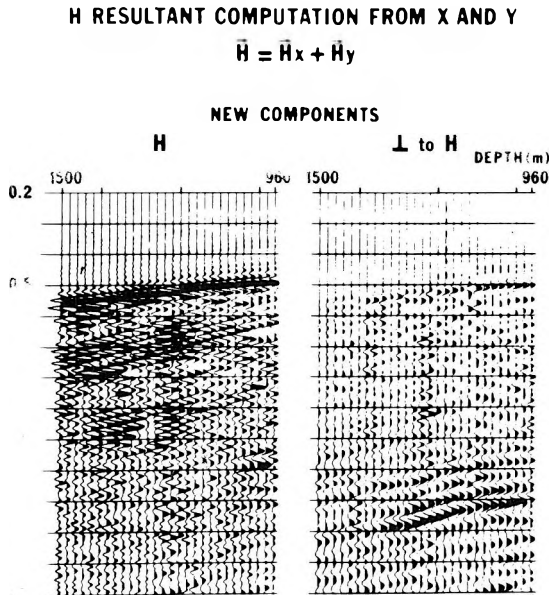
H RESULTANT COMPUTATION FROM X AND Y

$$\vec{H} = \vec{H}x + \vec{H}y$$

NEW COMPONENTS

Fig. 3. Horizontal resultant (*H*) and its perpendicular component from hodograph derived on first *P*-arrival

3. ábra. Az elsődleges *P* beérkezésre meghatározott hodográfból számított vízszintes eredő (*H*) és az erre merőleges vízszintes komponens

Рис. 3. Горизонтальная результирующая (*H*), рассчитанная по годографу, выведенному для первичных вступлений продольных волн, и перпендикулярная к ней горизонтальная компонента.

2. Estimation of polarization directions

Using the *Z* and *H* components, it is easy to define the polarization direction of the direct *P*-arrival. First the time (t_1) of the direct travel path of the *P*-wave from source to receiver is picked.

Then the construction of a hodograph yields the angle *AG* between the polarization direction of the downgoing *P*-wave and the vertical *(Fig. 4.)* We may infer from the first *P*-arrival the sketch of the propagation directions of the four types of waves *(Fig. 5)* and the diagram of the polarization directions *(Fig. 6)*. Supposing that we have roughly $V_P = 2V_S$, the angle β of the direction of propagation of *S*-wave is given by:

$$\sin \beta = \frac{1}{2} \sin \alpha.$$

At time t_1, if α_1 is the polarization angle of the downgoing *P*-wave measured on the hodograph:

— the polarization angle of the upgoing P-wave is $(-\alpha_1)$
— the polarization angle of the converted downgoing P–SV is $(\pi/2+\beta_1)$
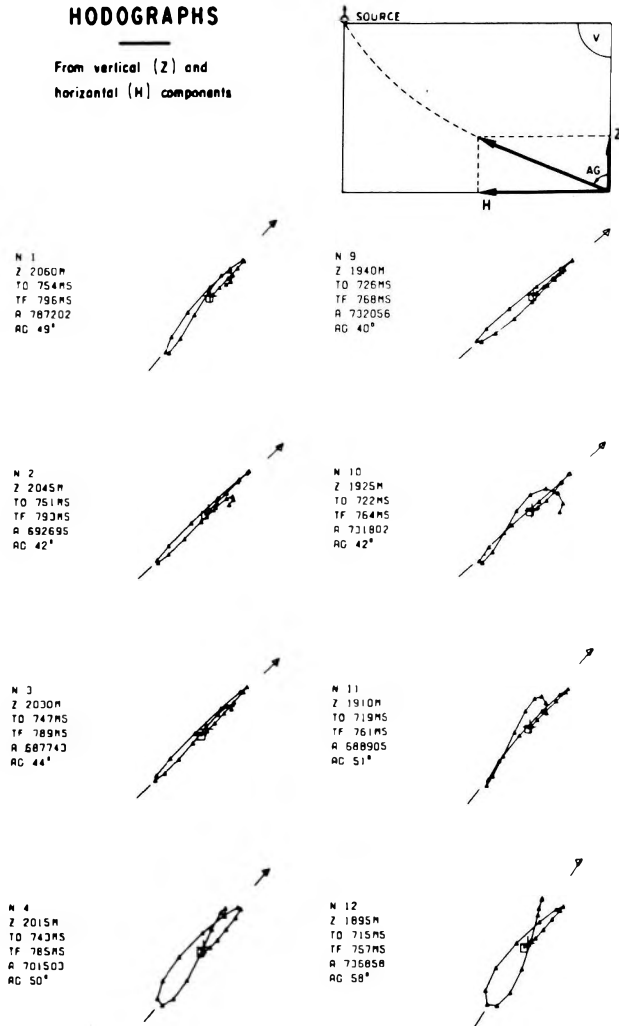— the polarization angle of the converted upgoing P–SV is $(\pi/2-\beta_1)$

HODOGRAPHS

From vertical (Z) and
horizontal (H) components

Fig. 4. Hodographs derived from Z and H components

Z — depth; TO — time of first break; TF — time of last sample; AG — angle of polarization

4. ábra. A Z és H komponensekből levezetett hodográfok

Z — mélység; TO — első beérkezés ideje; TF — utolsó mintavétel; AG — a polarizációs szög

Рис. 4. Годографы, выведенные из компонент Z и H

Z — глубина; TO — начальный момент времени; TF — конечный момент времени; AG — угол поляризации.
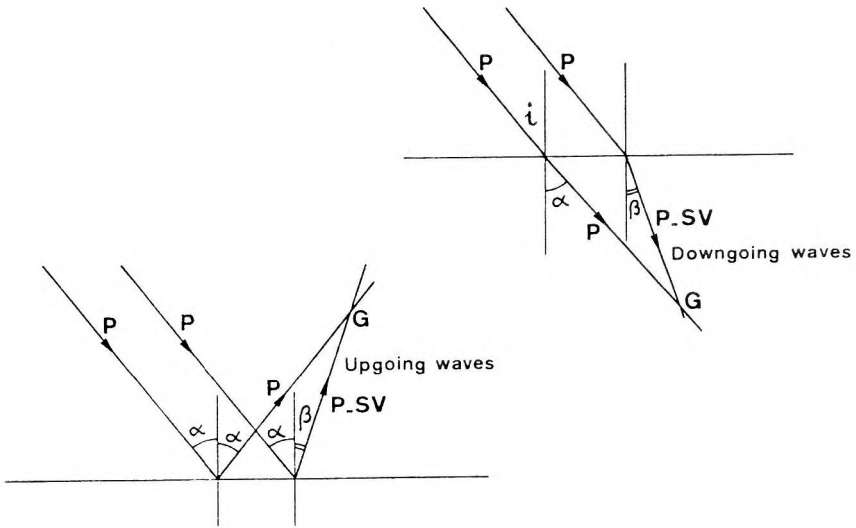
Fig. 5. Schematic of the ray paths close to the geophone for the four main types of waves. Downgoing waves: *P* and converted *SV*; upgoing waves *P* and *SV*

5. ábra. A geofonhoz közeli sugárutak vázlata a négy fő hullámtípusra. Lefelé haladó hullámok: *P* és konvertált *SV*; felfelé haladó hullámok: *P* és *SV*

Рис. 5. Схема лучевых путей вблизи от сейсмоприемника для четырех основных типов волн: нисходящих *P* и преобразованных *SV*, а также восходящих *P* и *SV*.
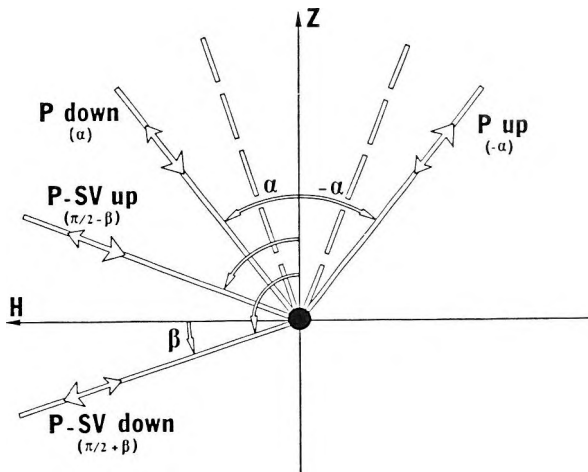
ASSUMPTION : $V_P/V_S = 2 \implies \sin\beta = 0.5 \sin\alpha$

Fig. 6. Directions of polarization relating to the wave modes close to the first *P*-arrivals

6. ábra. Polarizációs irányok az elsö *P* beérkezésekhez közeli hullámfajtákra

Рис. 6. Направления поляризации для волн, близких к первым вступлениям продольных волн.

Third, the polarization angles are estimated as a function of time. In the case of a constant velocity V_P (reflection coefficients are then derived from density variations), a simple relationship is found for both up- and downgoing P-waves:

$$\sin \alpha_i = \frac{t_1}{t_i} \sin \alpha_1$$

which yields the value of the polarization direction versus time. Simple formulae also lead to the estimation of polarization angles for $P\text{–}SV$-downwaves and $P\text{–}SV$-upwaves.

To be realistic, we chose a model with a given V_P velocity at the receiver level and a low varying average velocity from the surface, still with $V_P = 2V_S$. The estimates of the simplified model of constant velocity are still valid. The study was made with the following source offset to depth ratios: 0.25, 0.5, 1.0 and 1.5, and the following interval velocity (at geophone depth) to RMS velocity ratios: 0.5, 1.0, 1.5 and 2.0. *Figure 7* illustrates the raypaths with an equal distance for the source offset and the geophone depth; the velocity ratio is 1.5
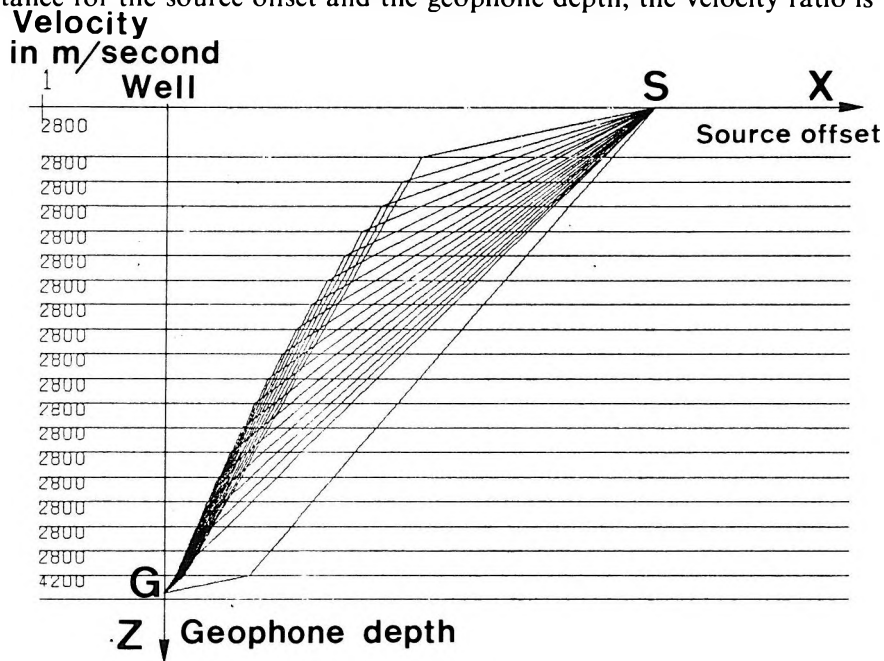

Fig. 7. Example of raytracing modelling for converted downgoing wave. Interval velocity at geophone depth is 4200 m/s, average velocity is 2800 m/s

7. ábra. A sugárkövetéses modellezés példája konvertált lefelé haladó hullámra. A geofon mélységében az intervallum sebesség 4200 m/s, az átlagsebesség 2800 m/s

Рис. 7. Пример моделирования путем прослеживания лучей для нисходящей преобразованной волны. На глубине сейсмоприемника интервальная скорость составляет 4200 м/с, а средняя скорость — 2800 м/с.

giving 4200 m/s for the interval velocity at the geophone and 2800 m/s for the average velocity. *Figure 8* shows the graph of the estimates of polarization directions plotted against time for the four types of waves.

ANGLES OF DIRECTIONS OF POLARIZATION

VERSUS TIME.   ASSUMPTION VP/VS = 2 $\implies$ sin β_1 = 0.5   sin α_1
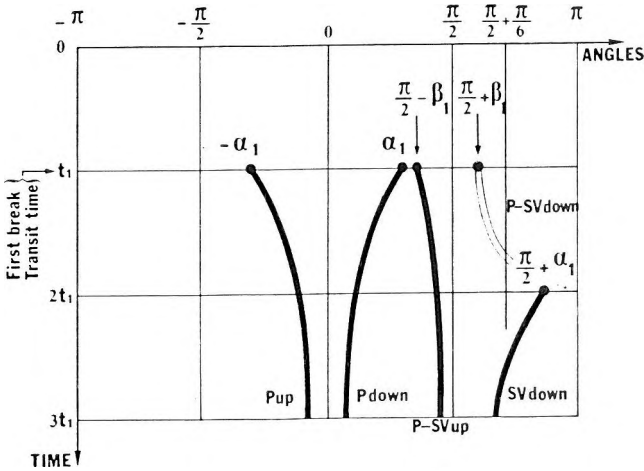
Fig. 8. Angles of wave polarization versus time for the different wave modes

8. ábra. Hullámpolarizációs szögek az idő függvényében, különböző hullámfajtákra

Рис. 8. Углы поляризации волн в зависимости от времени для различных типов волн.

3. Principle of wave separation

The coordinate system is changed so that a given type of wave is entirely determined by one of the components of the new system. The orthogonal component then only contains the projections of the other types of waves. For instance, from the fixed (Z, H) system of coordinates, we may choose the time variant system constituted by the P-downwave and its perpendicular direction. An $f–k$ bandpass filter over the P down direction will provide the P down component. An $f–k$ rejection filter over the same direction will provide two time-variant orthogonal components which only contain the other types of waves. We may then proceed with time-variant changes of coordinates and $f–k$ filtering to isolate a new type of wave, and yield two other time-variant orthogonal components which will only contain two types of waves.

In practice, the most energetic downgoing P and downgoing $P–SV$ events are progressively eliminated so as to recover two orthogonal components which only include upgoing P- and $P–SV$-waves. These waves are then separated by

a simple change of coordinates. The flowchart and the diagrams of the different systems of coordinates illustrate all the successive stages of the algorithm *(Fig. 9)*.
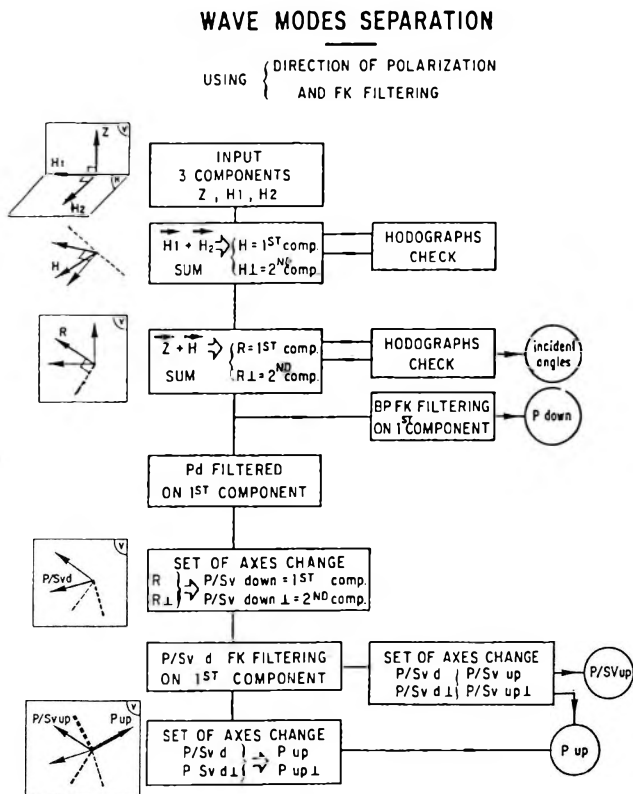
WAVE MODES SEPARATION

USING { DIRECTION OF POLARIZATION AND FK FILTERING

Fig. 9. Processing flowchart for wave field separation

9. ábra. A hullámtér szétválasztás folyamatábrája

Рис. 9. Схема процесса расчленения волнового поля.

4. Examples

The first example shows the wave field separation applied to offset VSP data. The downhole tool housed a three-component orthogonal geophone and the data were recorded from 1500 m to 960 m every 20 meters. A vibrator located at 1200 m from the wellhead was used as a seismic source.

First, hodographs are derived from a small window a few tens of milliseconds wide near the f rst *P*-arrival and the angle α of the polarization direction is calculated. This processing phase is important since the quality of the separation depends on the accuracy of determination of the angle α. It is very interesting to compare the angle values with the velocities derived from the sonic

log *(Fig. 10)*. Their validity can then be estimated, and questionable measurements can possibly be eliminated.

INTERVAL VELOCITY FROM SONIC LOG
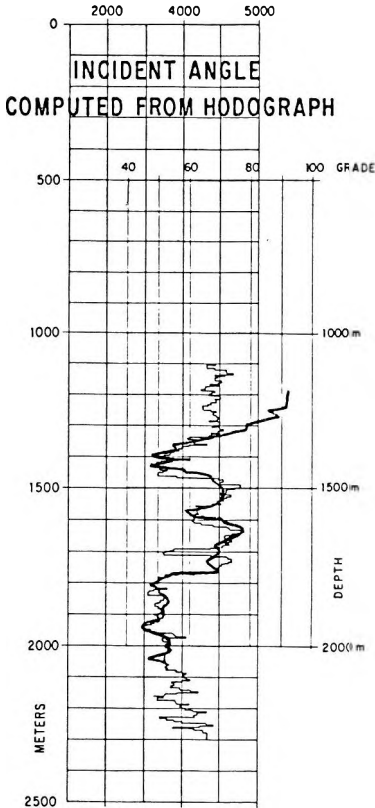

Fig. 10. Comparison of the incident angles (thick line) obtained from hodographs (Z and H components) with the sonic log velocity (thin line)

10. ábra. A hodográfból (Z és H komponens) számított beesési szögek (vastag vonal) összehasonlítása a szónikus intervallum sebességgel (vékony vonal)

Рис. 10. Сопоставление углов вхождения (жирная линия), рассчитанных по годографам (компонент Z и H), с акустической интервальной скоростью (тонкая линия).

The downgoing *P*- and *P–SV*-waves are separated after the process described above. The first change in coordinates is performed from the fixed (*Z, H*) system to the time-variant system constituted by the direction of the downgoing *P*-wave (*R*) and its perpendicular direction to facilitate rejection of the downgoing *P*-waves *(Fig. 11)*. The second change in coordinates is performed from the preceding system to the time-variant system constituted by the direction of polarization of the downgoing *P–SV*-wave and its perpendicular direction, to facilitate rejection of the downgoing *P–SV*-waves.

The results of the separation applied to the *Z* and *H* components *(Fig. 2)* are shown in *Figs. 12* and *13*. We notice in Fig. 13/b a residual downgoing *P–SV*-wave which is probably associated with elliptic polarization. Rejection on one component only is not sufficient in this case. Figure 13 is displayed with + 9 dB gain to improve visibility.
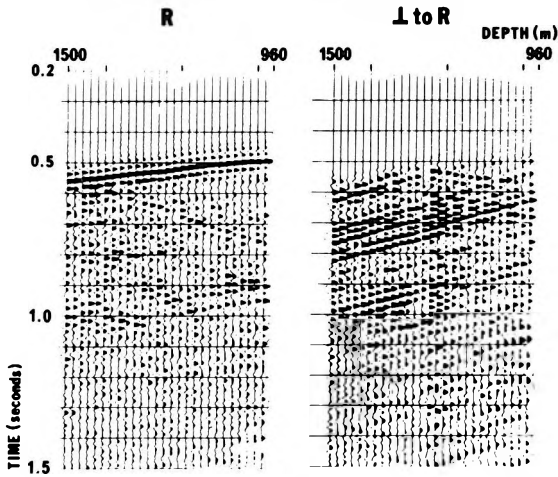
Applying three-component records in wave field separation   33

Fig. 11. New components after rotation of axes, polarized in the direction of the downgoing P-wave and its perpendicular component

11. ábra. A tengelyek elforgatásával keletkező új komponensek a lefelé haladó P-hullám irányába és az arra merőleges irányba polarizálva

Рис. 11. Новые компоненты, возникающие при повороте осей, поляризованные в направлении нисходящей продольной волны и перпендикулярно к ней.
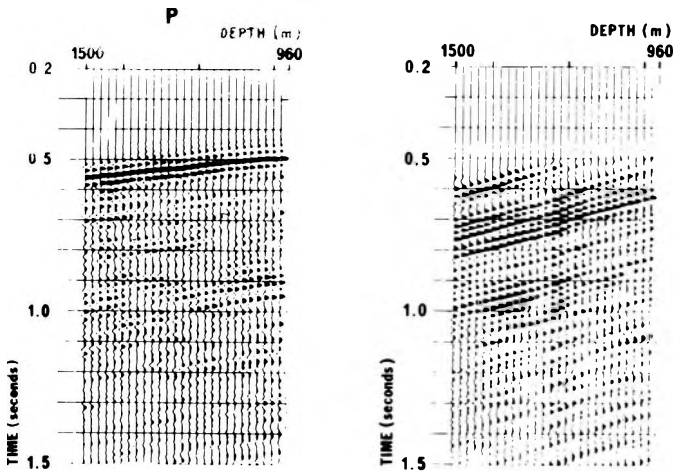
Fig. 12. Wavefield separation: downgoing P- (left) and SV-waves (right) after rotation of axes and f–k filtering

12. ábra. Hullámtér szétválasztás: lefelé haladó P- (bal oldalon) és SV-hullám (jobb oldalon) a tengelyek elforgatása és f–k szürés után

Рис. 12. Расчленение волнового поля: нисходящие волны P (слева) и SV (справа) после поворота осей и f–k фильтрации.

Figures 14 to 16 illustrate the main steps of this method on another VSP data set with greater offset. The vibrator was located 1775 metres from the wellhead, and the geophone spacing was 30 meters from 2060 m to 1100 m.

Figure 14 shows the 3 components of the raw VSP data. We should note that for the shallowest geophones, the first P-arrivals can only be seen on the horizontal components (*H*1, *H*2) because of large angles of incidence. *Figures 15* and *16* show the results of the separation.
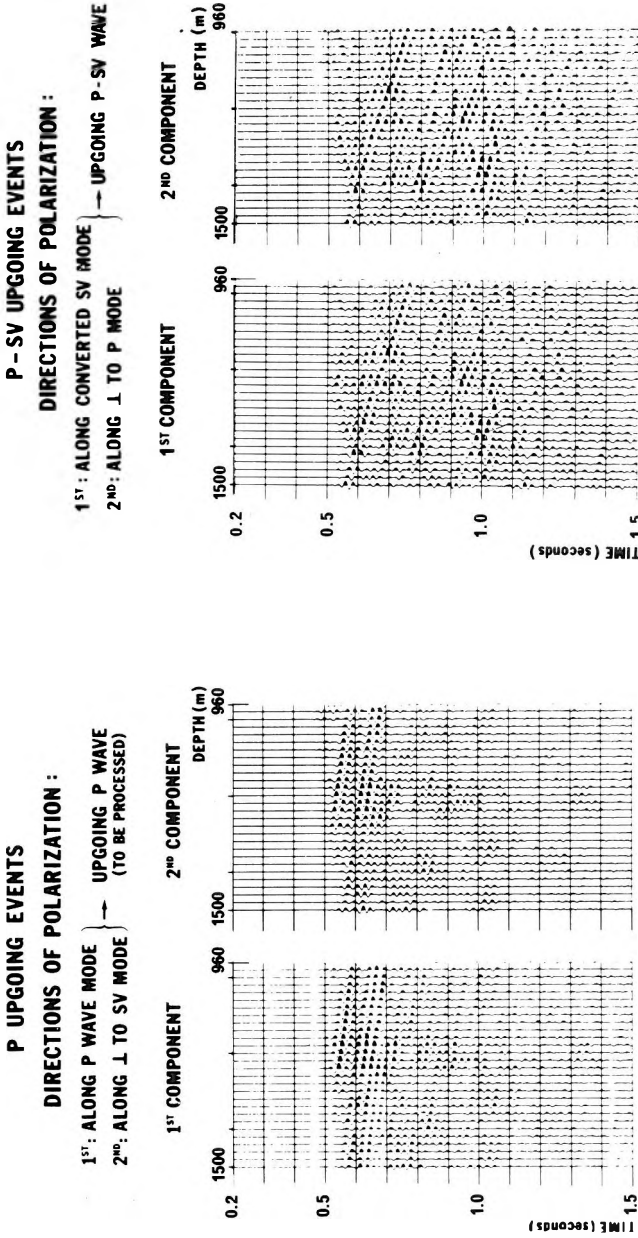
Fig. 13. Wave field separation: upgoing *P*-wave (left) and upgoing converted *SV*-waves (right)

13. ábra. Hullámtér szétválasztás: felfelé haladó *P*-hullám (bal oldalon) és konvertált *SV*-hullám (jobb oldalon)

Рис. 13. Расчленение волнового поля: восходящие волны *P* (слева) и преобразованные волны *SV* (справа)
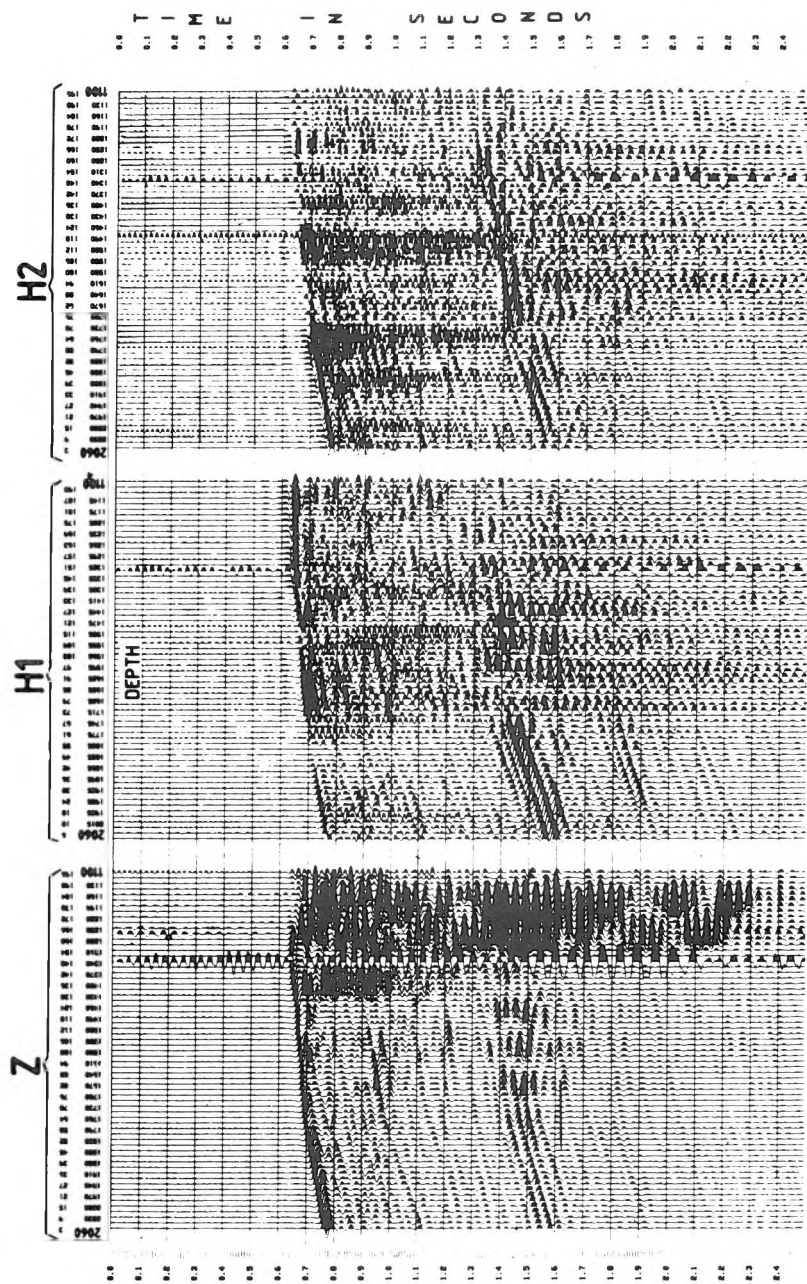
Fig. 14. Three-component VSP raw data: vertical and horizontal components. Geophone levels from 2060 m to 1100 m below KB. Vibrator 1775 m from wellhead, sweep 13–100 Hz

14. ábra. Háromkomponenses VSP felvételek: függőleges és vízszintes komponensek. Geofon szintek 2060 m-től 1100 m-ig a forgatóasztal szintje alatt. A vibrátor a fúrás helyétől 1775 m távolságra volt, vibrojel 13–100 Hz

Рис. 14. Трехкомпонентные записи БСП вертикальные и горизонтальные компоненты. Уровни сейсмоприемников — с 2060 м до 1100 м под ротором. Вибратор находился в 1775 м от скважины, вибросейсмический сигнал — с 13 гц до 100 гц.

DOWNGOING WAVES
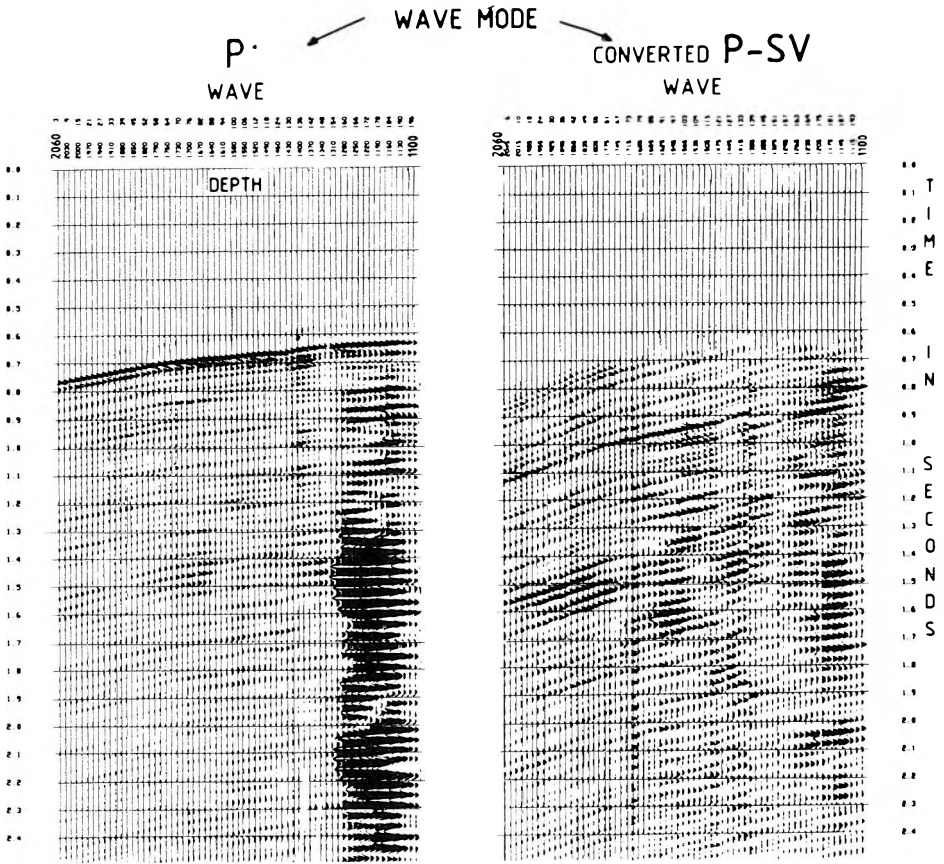AFTER SEPARATION
- SET OF AXES ROTATING
- FK FILTERING ON DOWNGOING

Fig. 15. Downgoing P- and converted SV-waves after time variant wave field separation:
rotation of axes and f–k filtering

15. ábra. Lefelé haladó P- és konvertált SV-hullámok, időben változó hullámtér-szétválasztás
után: tengelyek elforgatása és f–k szürés

Рис. 15. Нисходящие волны P и преобразованные волны SV после расчленения волнового
поля с изменением во времени: поворот осей и f–k фильтрация.

UPGOING WAVES
AFTER SEPARATION

{
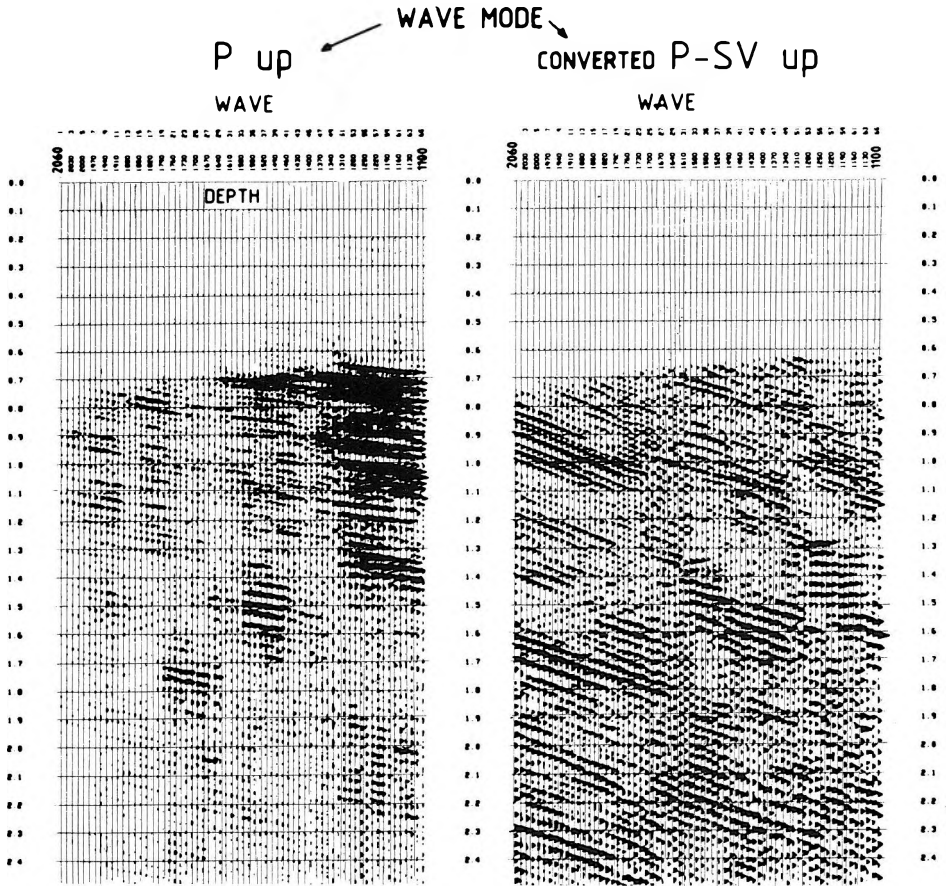- SET OF AXES ROTATIONS
- FK FILTERING ON DOWNGOING
  P AND P-SV WAVES
}

WAVE MODE

P up   CONVERTED P-SV up

WAVE   WAVE

Fig. 16. Upgoing *P-* and converted *SV*-waves after time-variant wave field separation

16. ábra. Felfelé haladó *P-* és konvertált *SV*-hullámok, időben változó hullámtér-szétválasztás után

Рис. 16. Восходящие волны *P* и преобразованные волны *SV* после расчленения волнового поля с изменением во времени.

Comparison between two corridor stacks derived from zero-offset upgoing *P*-events and upgoing converted *SV*-events is illustrated in *Fig. 17*. *SV*-waves have been separated as stated above then plotted versus *P* traveltime by using the relationship between *P* and *S* times picked from zero-offset VSP data.
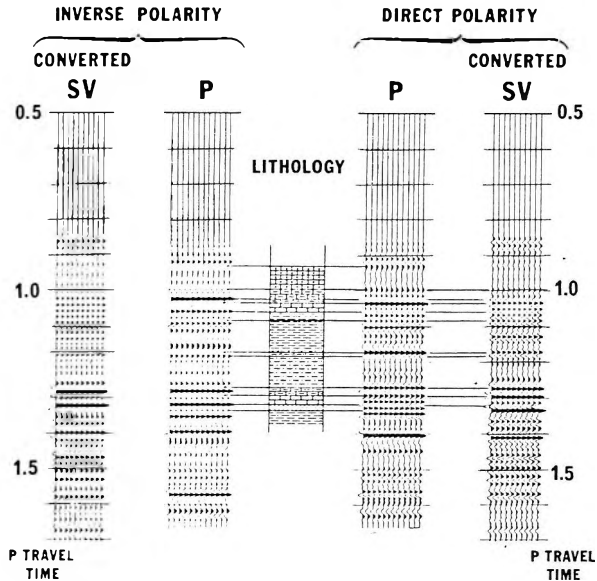

Fig. 17. Application of converted upgoing shear wave by comparison with upgoing *P*-waves with the same time-scale and related lithology

17. ábra. Konvertált felfelé haladó nyíró hullám alkalmazása felfelé haladó *P*-hullámokkal való összehasonlításra, azonos időlépték és a megfelelő rétegsor esetén

Рис. 17. Сопоставление преобразованных восходящих поперечных волн с восходящими продольными волнами в случае тождественных временных масштабов и подходящей литологической колонки.

5. Conclusion

The algorithms we have described proved efficient and robust in industrial applications as shown by many examples. The use of time-variant changes in coordinates seems to bring an improvement with respect to tests carried out with constant polarization angles plotted against time.

We may proceed separately for the processing of each type of wave. The wave field separation and the processing of the upgoing converted *SV*-waves up to the corridor stack provide a VSP log of *P–SV*-waves. This *P–SV* converted wave log is particularly interesting as the converted wave surface recording keeps developing and comparison between the "converted wave" section and

the *P–SV* converted wave log should facilitate overall interpretation. However, the main advantage is to improve the quality of later stages of the processing, in the case of Vertical Seismic Profiles with large offsets. We will summarize our experience as follows:

— for small offsets, seismic response is obtained from the *Z*-component only,
— for average offsets, the processing addresses the vertical component too, but the total wave (*R*) is used to find the downgoing signal that is useful for deconvolution,
— for large offsets, the energy of upgoing and downgoing *S*-waves becomes very great. Processing then demands more accurate separation as described above.

HÁROMKOMPONENSŰ FELVÉTELEK ALKALMAZÁSA HULLÁMTEREK SZÉTVÁLASZTÁSÁRA

R. DAURES és P. TARIEL

A lyukszáji gerjesztésű VSP méréseknél a hullámtér csak felfelé és lefelé haladó *P*-hullámokat tartalmaz, melyek csak vertikális (*Z*) komponensekből állnak. Ha a gerjesztés távolabb van, a hullámtér bonyolultabbá válik a konvertált *P–SV*-hullámok jelenléte miatt, melyek a *P*-hullámoktól eltérnek mind látszólagos sebességükben, mind polarizáltsági irányukban. A szeizmika ettől fogva nem skaláris, hanem vektoriális jellegű, és emiatt három komponensű felvételekre van szükség.

Az első beérkezésekre a hodográf megadja a *P*-hullám polarizációs irányát. A *P–SV*-hullámok polarizációs irányát 2:1 arányú *P–S* sebességhányados feltételezésével becsüljük. A tengelyeknek a polarizációs irányokhoz viszonyított változtatásai és a látszólagos sebességekhez kapcsolt *f–k* szűrés együttes alkalmazása lehetővé teszi a teljes hullámtér felosztását az alábbi négy hullámtípusra: lefelé haladó *P*, felfelé haladó *P*, lefelé haladó *P–SV*, és felfelé haladó *P–SV*-hullámok.

ПРИМЕНЕНИЕ ТРЕХКОМПОНЕНТНОЙ ЗАПИСИ В РАСЧЛЕНЕНИИ ВОЛНОВЫХ ПОЛЕЙ

Р. ДОР и П. ТАРЬЕЛ

При измерениях методом вертикального сейсмического профилирования (ВСП) с возбуждением волн на устье скважины волновое поле состоит исключительно из восходящих и нисходящих продольных волн, содержащих одни вертикальные компоненты (*Z*). При перемещении точки возбуждения на некоторое расстояние от скважины волновое поле становится более сложным в связи с появлением преобразованных *P–SV* волн, отличающихся от продольных (*P*) волн как в кажущейся средней скорости, так и в направлении поляризации. С этого момента сейсморазведка вместо скалярной становится векторной, поэтому возникает необходимость в трехкомпонентных записях.

В отношении первых вступлений по годографу определяется направление поляризации продольных волн. Направление поляризации волн *P–SV* оценивается на основе предположения, что отношение скоростей волн *P–SV* составляет 2:1. Изменение осей по отношению к направлениям поляризации, а также совместное применение *f–k* фильтрации в связи с кажущимися скоростями делают возможным расчленение полного волнового поля на нижеследующие четыре типа волн: нисходящие продольные, восходящие продольные, нисходящие *P–SV* и восходящие *P–SV*.